Section: Research Paper

Structural, Optical and Electrical properties of Ruthenium doped V_2O_5 thin films by deposition method

A. Sherin Fathima[1], I.Kartharinal Punithavthy[1*], S.Johnson Jeyakumar[1], B. Arunkumar[2], A. Muthuvel[3,4]

[1]Department of Physics, T.B.M.L College (Affiliated to Bharathidasan University, Tiruchirapalli-620024), Porayar 609 307, Nagapattinam, Tamil Nadu, India.

[2]Sir Issac Newton College of Engineering and Technology (Affiliated to Anna University – Chennai), Nagapattinam, Tamil Nadu, India.

[3]Department of Physics, Faculty of Science and Technology, Airlangga University, Surabaya 60115, Indonesia

[4]Department of Physics, Theivanai Ammal College for Women (Autonomous), Villupuram, Tamil Nadu – 605602, India

*Corresponding Author: profpunithaphysics@gmail.com

Abstract

Nowadays, Semiconducting thin films are efficient candidates for good optical and electrical properties. In this present study, thin films of Ruthenium-doped V_2O_5 with different weight percentages (2% to 8%) were prepared through the method of spray Pyrolysis. The prepared Ru doped thin films were characterized by spectrographic tools such as XRD, SEM with EDAX, FTIR, UV-Vis and Hall effect to study their crystalline nature, Functional group, band gap, resistivity, conductivity and mobility of the flow of electrons respectively. The structural morphology of the synthesized thin films was discussed through the micrographic image obtained from Scanning electron microscopy together with their surface occupancy plots. The obtained minimum crystallite size is about 24.8 nm for 8% molarities. The morphological and structural studies show enhanced results for an 8% sample which makes it a viable candidate for optical and electrical applications.

Keywords: Spray Pyrolysis, V_2O_5 Thin films, Surface Morphology, Ruthenium, and Electrical Properties.

1. Introduction

Nowadays, thin films of V_2O_5 have gained noteworthy attention in the microelectronic world [1]. In recent years, vanadium oxides play a vital role due to their sensing activity, selective catalytic and potential applications in electrochemical capacitors [2-5]. And also vanadium oxide thin film has a scientific and technological application which includes electro chromic devices (ECD), toxic gas detectors, electronic and optical switches [6-8]. Vanadium oxides have interesting electronic structures is $3d^3 4s^2$ electrons in their outer shell, which enables

them to be in different oxidation states such as V^{2+}, V^{3+}, V^{4+} and V^{5+}. This creates complex as well as challenging material. In different vanadium oxides, vanadium pentoxide (V_2O_5) is widely used and is stable. The direct band gap of V_2O_5 makes V_2O_5 thin films lay footprints in photo detection applications which leads to the utilizing V_2O_5 thin films in optoelectronic devices [9]. However, pure crystalline V_2O_5 generally possess an orthorhombic structure that comprises better chemical property and good specific energy with thermal stability [10]. Because of the mentioned properties of V_2O_5 crystal's orthorhombic structure, these V_2O_5 thin films and their related materials were used for fabricating IR detectors, solar cells and sensors too.

V_2O_5 thin film has been synthesized using various methods such as sputtering [11], sol-gel method [12], hydrothermal [13], pulsed laser deposition [14], chemical vapor deposition [15] and co-precipitation technique [16], etc. Among, these various deposition techniques, the thermal evaporation method is the most predominant. The thermal evaporation technique is the most challenging versatile method for the deposition of V_2O_5 thin films.

However, High surface area V_2O_5 aerogels exhibit a larger lithium intercalation capacity compared to crystalline V_2O_5. Hence, a major difficulty of these electrodes is their limited long-term cycling stability. To overcome the specific rate, intercalation rate and cycling performance of vanadium oxide metal such as $M_XV_2O_5$ (M= Zr, Ag, Ru, etc.) have been taken to be used as cathode materials due to their unique structure. Moreover, there is no report so far of V_2O_5 particles doped by Ruthenium in lithium-ion batteries at high deposition temperatures. In the present work, pure and Ruthenium doped V_2O_5 thin film in various molar percentages [2%, 4%, 6% and 8%] were deposited. These prepared thin films were synthesized by the spray pyrolysis technique.

The obtained pure and Ruthenium doped V_2O_5 thin film (with 2, 4, 6% of Ruthenium) were characterized by X-ray diffraction (XRD) for structural analysis, scanning electron microscope (SEM) was used to examine the surface morphology and the electrical studies hall effect were also recorded to find the conductivity of the prepared thinfilms.

2. Experimental Procedure

V_2O_5 thin films were prepared onto ITO substrates by spray pyrolysis of pure V_2O_5 Powder from an electrically heated molybdenum boat kept at ~ 1823 K in a vacuum very good than 8 x 10^{-6}Torr. A Hind High Vacuum 12A4 Coating was used for the deposition of the experimental thin films. A diffusion pump backed by a rotary pump was carried to produce the pressure of 3 x 10^{-6}Torr. Well-Polished ITO substrates were mounted on a copper holder which was fixed on a tripod in the bell jar. After getting the ultimate vacuum of 5 x 10^{-6}Torr and the desired substrate temperature in the chamber, the glow discharge was initiated further ionically polished the substrates in the vacuum chamber. This process was done for two minutes. The system was allowed to reach the ultimate vacuum so that the crystalline nature of Ru doped V_2O_5 thin films can be enhanced. When the power was fed to

the boat, the material in the boat evaporated and the vapors reacted with the oxygen gas leading to film deposition on the substrate. The temperature of the boat during deposition was monitored using an optical pyrometer [17]. The substrates were sustained at the required deposition temperature and the molybdenum boat in which Ruthenium (Ru) doped V_2O_5 powder with different weight percentages kept. The shutter covering the substrates was opened when the required temperature of the boat reached about 1823 K and it was maintained during the deposition of the films.

The well-adherent V_2O_5 films underwent structural, morphological and optical studies. The structural properties characterization by X-ray diffraction is carried out using X'Pert High Scorer-P analytical Diffractometer with Cu-K radiation of wavelength (1=5406Å). The morphology was analyzed by Scanning Electron Microscope (Hitachi S-4500 SEM machine). The spectroscopic vibration studies of Ru doped V_2O_5 thin films have been performed on FTIR (PerkinElmer L1600) between the wavenumber range of 400–4000 cm^{-1}. The optical studies evolved using UV spectrophotometer, and the wavelength was prescribed from 200 to 800 nm. And the Electrical studies were carried out using the Hall Effect.

3. Result and Discussion

3.1 Structural Analysis

XRD patterns of pure and Ruthenium doped V_2O_5 thin films with different weight percentages (2%, 4%, 6% and 8%) are shown in Fig. 1. The obtained thin films reveal characteristic peaks related to orthorhombic phase crystal structure. The noticed peaks are gently matched with standard patterns of JCPDS card No. 89-2482 and the peaks 20.85, 30.00, 34.97, 50.27,55.02, and 59.80 at crystal plane (101), (012) and (312) respectively [18-20]. The crystallite size of the prepared Ru doped thin films was calculated using Debye's Scherrer formula [21],

$$D = \frac{K\lambda}{\beta Cos\theta} \qquad \text{---------[3.1]}$$

Where K is a Scherrer constant, λ is the wavelength of the beam, β is (FWHM) and θ is Bragg's diffraction angle. The average crystallite size of the prepared thin films decreases from 29.5 to 22.2nm with the increase in weight percentage, which is due to the different ionic radii of Ru and V_2O_5. Compared with the pure V_2O_5, the minute peaks disappeared, when increasing the weight percentage [19]. However, the average dislocation density and Average microstrain of the prepared thin films are increased linearly with the increase of weight percentages.

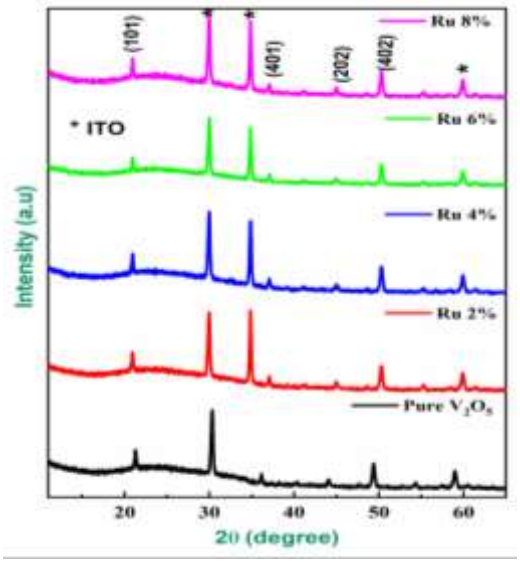

Fig. 1 XRD patterns of pure V_2O_5 with different weight percentages

Table1 Structural parameters of pure V_2O_5 with different weight percentages

S. No	Sample	Average crystallite size, $DX10^{-9}m$	Average Dislocation density, $(X10^{14}m)$	Average Micro strain, ε $X10^{-3}m$
1	V_2O_5	29.5	1.14061E+15	0.00122
2	2%	28.3	1.2461E+15	0.00138
3	4%	26.8	1.38471E+15	0.00154
4	6%	24.6	1.52471E+15	0.00184
5	8%	22.2	1.65471E+15	0.00213

3.2 Morphology Studies

3.2.1 SEM Micrographs

SEM images of Ru-doped V_2O_5 with different weights percentages (2, 4, 6, and 8%) thin films are shown in Fig2. From Fig.2, the prepared thin films were spongy in shape with few agglomerations. The noticed spongy-like shape gets reduced in the increase of Ruthenium dopant percentage. The 8% Ru doped V_2O_5 thin film shows a smooth surface with plateless scattered on its Surface. In Fig 2, EDAX shows the confirmation of occurred elements such as Ruthenium, vanadium, and oxide with their appropriate atomic ratio. There is no secondary phase of impurity.

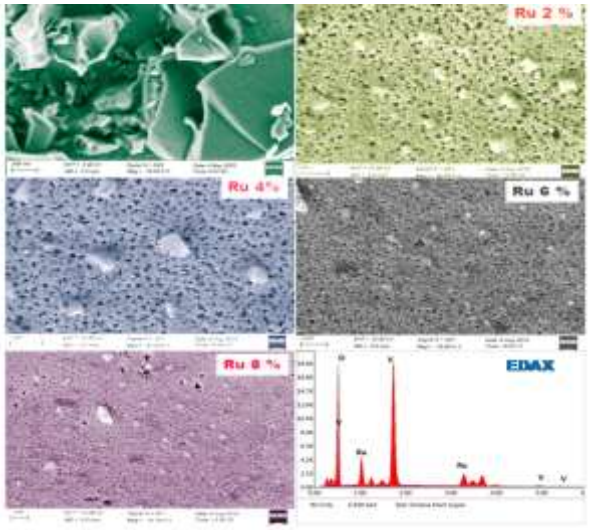

Fig 2. SEM with EDAX images of Ru-doped V_2O_5 with different weight percentages

3.2.2 Surface Occupancy plots

Furthermore, we intended to illustrate the surface micro structural condition of pure and varied percentages of Ruthenium ion-doped V_2O_5films, as seen in the previous SEM photographs. Here, the surface condition was demonstrated with the aid of a surface occupancy plot through image J. thin film samples have been shown in Fig 3(a-e) to illustrate the surface occupancy state. To begin, to compare the outcomes of the SEM compared with those of the SOP, in the case of pure V_2O_5 thin film, the SEM reveals a peeled micro structural condition along with crippled and aggregated conditions, as shown in Figure3. The SOP reveals that the signals must be intensified in certain regions due to the microstructures' clumping. However, after incorporating 2%, 4% and 6% of Ru-ions into the V_2O_5, the surface morphology was radically transformed, as depicted in Fig.3(b-d), exhibiting pinholes – (micro channels) appearing in the scanning region. The mild, consistent signals with some strong signals due to minor agglomerations are visible in their SOP. After that, in the case of 8% of Ru-ion doped V_2O_5 SOP having very smooth and well-distributed signals with a reduction in micro structural sizes, as seen in Figure 3e. So, we infer that the current SOP study has appropriate evidence for the Ru-ions implications in host thin film. We suggest the vital thing about the pin-hole and void formations, which are acquired due to defects arising in crystalline V_2O_5while interrupting with dopant ions. As a result of the exterior diffusion of Ru-ions during specimen meets calcination in thin films, multiple stoichiometry vacancies can be created in this kind of cavity. The microstructural parameters in this instance of pin-holes are more advantageous for charge transfers, suggesting that they may operate as channels, resulting in improved electrical conductivity [22]. Ultimately based on the outcomes, it was found that various Ru-ions doped V_2O_5thin films were more useful for solar cell-based applications.

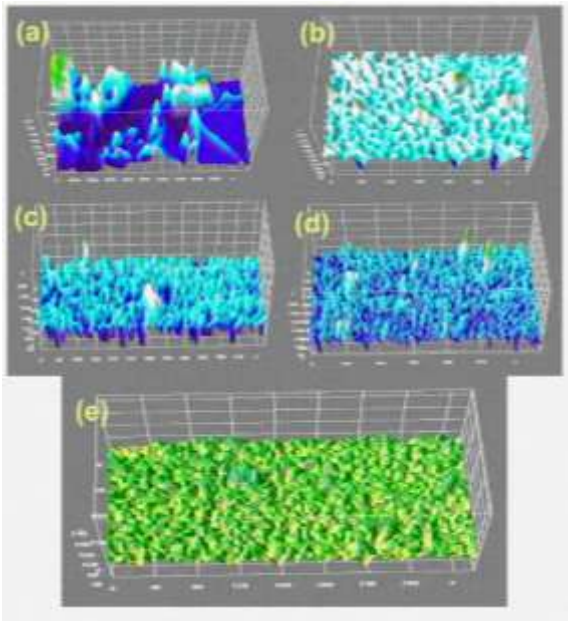

Fig. 3(a-e) Surface Occupancy plots of Ru-doped V_2O_5 with different weight percentages

3.3 Functional Studies

Fig.4 depicts the FTIR spectra of pure and varied percentages of Ruthenium ion-doped V_2O_5 films. The presence of functional groups in the produced thin films are further confirmed by the absorption of IR in molecular vibrations. The stretching vibration of the metal-oxide bond is represented by the vibrational frequency at 621cm^{-1}. Water molecules stretching vibration O-H bonds are responsible for the strong, intense peak at 3250 cm^{-1}. O-H bending vibration is responsible for the peak at 1310 cm^{-1}, which is caused by the calcinated thermal interfaces, on the other hand, the experimental reaction may be a factor for O-H molecule incorporation.[23].

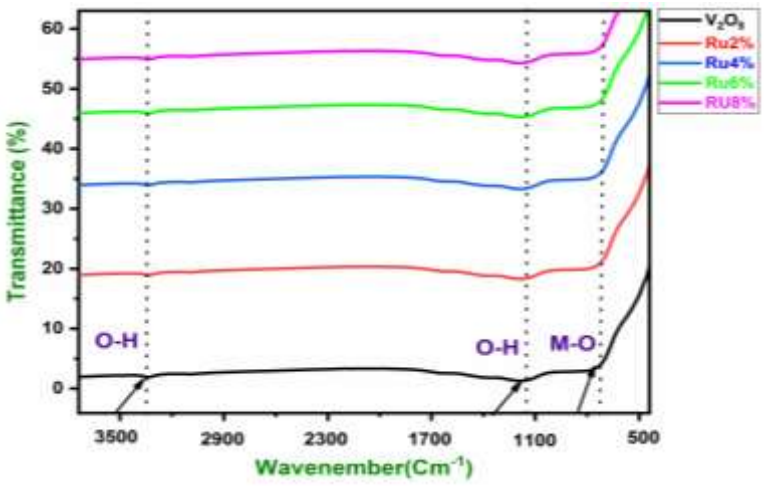

Fig.4 FTIR Spectra of Ru doped V_2O_5 with different weight percentages

Table 2. FTIR Spectra of Ru doped V_2O_5 with different percentages

S.NO	Vibrational assignments	Experimental absorption (cm^{-1})				
		V_2O_5	2%	4%	6%	8%
1	Metal - oxide	621	621	621	621	621
2	O - H bending vibration	1310	1310	1310	1310	1310
3	O - H stretching vibration	3250	3250	3250	3250	3250

3.4 Optical Studies

Figure 5 depicts the UV-Vis spectra of Ruthenium ion-doped V_2O_5 films with different weight percentages (2% to 8%). As the doping percentage rises, the absorbance decreases monotonously. The abrupt drops in transmittance are caused by the absorption of the majority of incoming photons with wavelengths between 300 nm and 800 nm. The region of fundamental absorption edge for ITO coated Ru doped V_2O_5 thin films with absorbance values of 325.6, 320.8, 317.4, 311.1 and 305.4 at 2% to 8% are depicted in Fig.5. The spectra show that the absorption edge indicates a red shift in wavelength as crystallite size decreases, which suggests a shift on the lower energy side. The microstructure and growth conditions of the films have an impact on the optical characteristics of ITO-coated Ru-doped V_2O_5 thin films with various weight percentages.

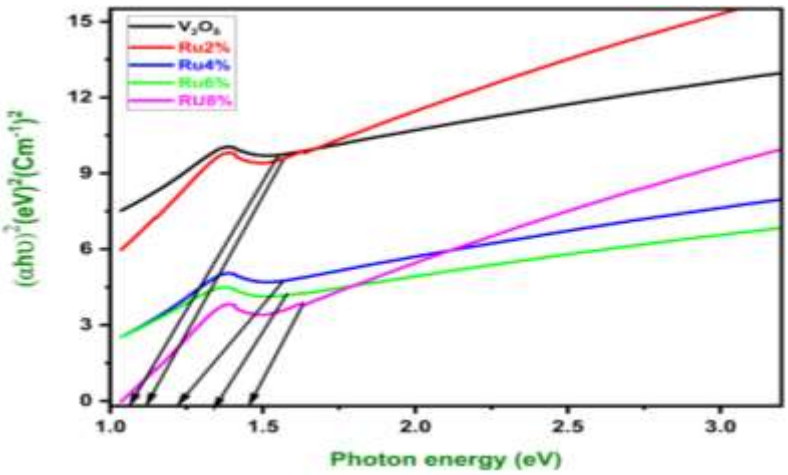

Fig. 5 Optical absorption spectra of Ru-doped V_2O_5 with different percentages

The optical band gap energies are 2.06, 2.11, 2.16, 2.28, and 2.39 eV. The band gap energies are increases with the increase in doping percentage which is agreed with the Brus equation [21]. Furthermore, the widening of bandgap in the prepared Ru-doped V_2O_5 thin films is due to the phenomenon of quantum size effects, which is higher for films at low growth temperatures, where the size of grains is relatively low (≤50nm). In addition, the mean crystal dimension becomes small; therefore, the quantum size effects lead to increase in the band gap. The defects in the lattice of Ru-doped V_2O_5 thin films are due to the oxygen vacancy between two V-O layers that create lower absorption bands in optical spectra. This oxygen vacancy is raised due to the disorders in atomic arrangement.

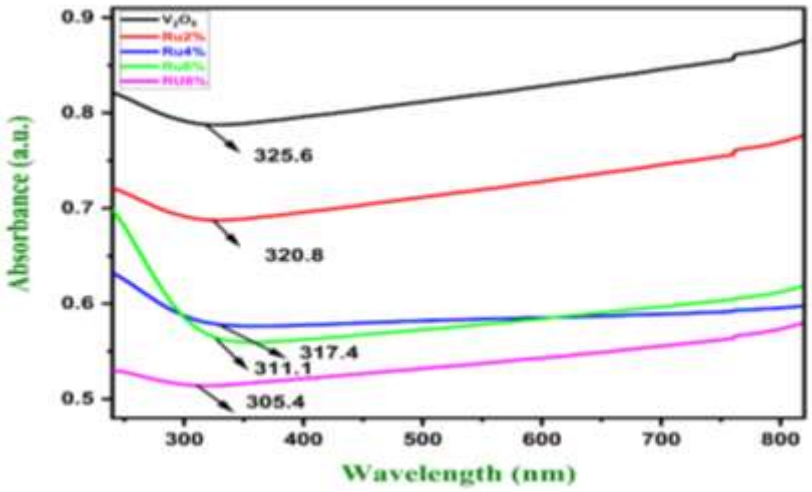

Fig. 6 Bandgap energy of Ru-doped V_2O_5 with different percentages

Table.3 Optical properties of Ru doped V_2O_5 with different percentages

Composition	Absorbance	Bandgap (eV)
V_2O_5	325.6	2.06
2%	320.8	2.11
4%	317.4	2.16
6%	311.1	2.28
8%	305.4	2.39

3.5 Electrical Studies

Hall Effect:

The transport parameters of the prepared samples were studied by using the Hall Effect at room temperature. The changes in the electrical transport because of increasing the dopant amount of Ruthenium in V_2O_5 thin films are summarized in the Table.4. The ions of vanadium show semiconducting features because of their different oxidation states due to the bouncing of 3d unpaired electrons. Fig. 7(a) shows the mobility and carrier concentration of

the pure V_2O_5 thin films and V_2O_5 thin films doped with (2,4,6 and 8%) of ruthenium. It shows that the mobility and carrier concentration increase for 2% of dopants and then it gradually decreases for 4, 6 and 8% of dopants.

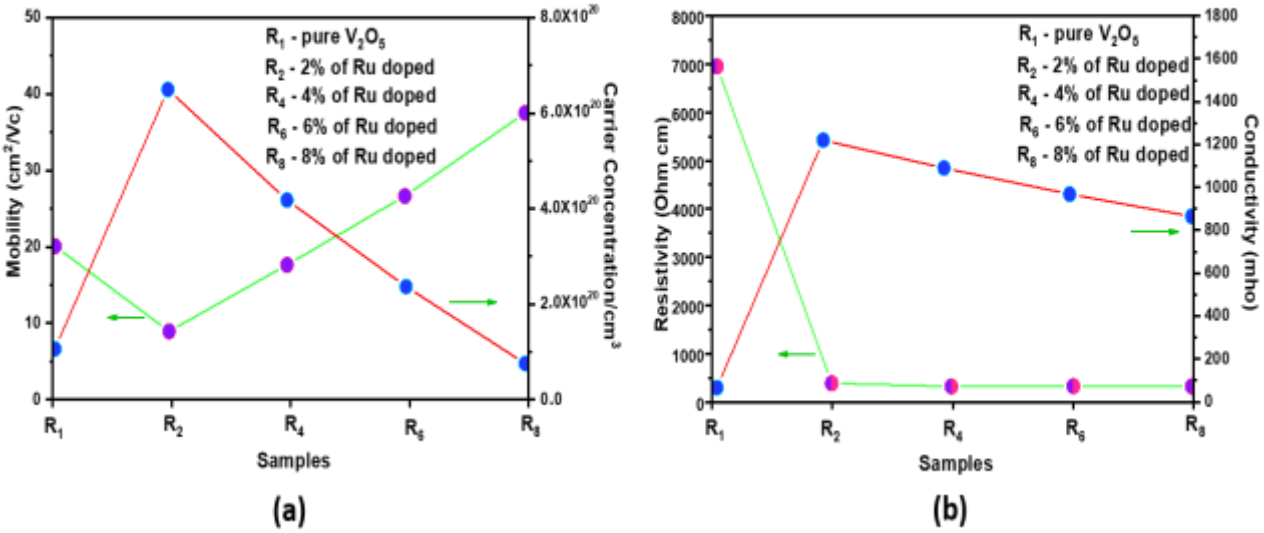

Fig. 7 Electrical studies of V_2O_5 thin films with different percentages

However, Fig. 7(b) shows the resistivity and conductivity of the pure V_2O_5 thin films and V_2O_5 thin films doped with (2, 4, 6 and 8%) of Ruthenium. which portrays that, the thin film's conductivity rises as a result of the creation of Oxygen vacancies. So, the Ruthenium inclusion on the V_2O_5 thin film matrix leads to a remarkable influence on the mobility of the prepared samples is revealed.

Table.4 Electrical parameters of V_2O_5 thin films with different percentages

Sample	Resistivity (ρ)(Ω cm)	Conductivity (σ)(Ω cm)$^{-1}$	Mobility (μ)(cm^2/Vs)	Carrier concentration/C m^3
R_0	$2.19x10^3$	$4.61x10^2$	$0.8\ x10^1$	$1.7\ x10^{20}$
R_2	$6.45x10^3$	$1.17\ x10^2$	$4\ x10^1$	$6.8\ x10^{20}$
R_4	$4.89x10^3$	$1.09\ x10^2$	$2.5\ x10^1$	$4.4X10^{20}$
R_6	$4.39\ x10^3$	$0.95\ x10^2$	$1.4\ x10^1$	$2.5X10^{20}$
R_8	$3.97\ x10^3$	$0.88\ x10^2$	$0.45\ x10^1$	$0.8X10^{20}$

4. Conclusion

The thin films of Pure V_2O_5 with different weight percentages (2, 4, 6and 8%) were prepared and coated in the ITO substrate by the method of spray pyrolysis. The XRD pattern shows the respective peaks of the prepared V_2O_5 thin films with orthorhombic structures. The average crystallite size of the Pure V_2O_5 and doped Ruthenium with different weight percentages (2, 4, 6 and 8%) are 29.5 to 22.2 nm respectively. It shows that the crystallite size decreases with the increase in weight percentages. The FTIR spectra show the appropriate bands of bonds present in the prepared samples, while the optical spectra show their corresponding absorption spectra with their respective band gaps, which indirectly shows the prepared material is a semiconductor. In addition, the SEM/EDAX micrographs show that the synthesized thin films were formed in the shape of crumbled paper for 8% of molar concentration. However, surface occupancy plots show that sheet-like particles are uniformly distributed over the scanning surface area. Hence, this present study suggests that V_2O_5 thinfilms prepared through spray pyrolysis with the increase in the dopant weight percentages enhance its optical and electrical properties, which may lead to use the prepared samples for effective optical and electrical applications.

References

1. Zhai, T., Liu, H., Li, H., Fang, X., Liao, M., Li, L., Zhou, H., Koide, Y., Bando, Y., & Golberg, D Centimeter-long V_2O_5 nanowires: from synthesis to field-emission, electrochemical, electrical transport, and photoconductive properties. Advanced materials, 22(23), 2547–2552 (2010). https://doi.org/10.1002/adma.200903586.
2. Y. Wu, G. Gao and G. Wu, Self-assembled three-dimensional hierarchical porous V_2O_5/graphene hybrid aerogels for supercapacitors with high energy density and long cycle life, J. Mater. Chem.A, 3, 1828 (2015). https://doi.org/10.1039/C4TA05537C.
3. Mu J, Wang J, Hao J, Cao P, Zhao S, Zeng W, Miao B and Xu S, 'Hydrothermal synthesis and electrochemical properties of V_2O_5 nanomaterials with different dimensions', Ceramics International, 41(10), 12626-12632 (2015).
4. Kodu, M.; Berholts, A.; Kahro, T.; Kook, M.; Ritslaid, P.; Seemen, H.; Avarmaa, T.; Alles, H.; Jaaniso, R. Beilstein, Graphene functionalized by laser-ablated V_2O_5 for a highly sensitive NH_3 sensor, J. Nanotechnol. 8, 571–578, (2017). https://doi.org/10.3762/bjnano.8.61.
5. K.Y. Pan and D.H. Wei, Optoelectronic and electrochemical properties of vanadium pentoxide nanowires synthesized by vapor-solid process, Nanomaterials, 6(8), 140, (2016). https://doi.org/10.3390/nano6080140.
6. O. Schilling and K.Colbow, A mechanism for sensing reducing gases with vanadium pentoxide films, Sens. Actuators B, 21 (2), 151-157 (1994). https://doi.org/10.1016/0925-4005(94)80017-0.
7. D.Wruck, S. Ramamurthi, and M. Rubin, Sputtered electrochromic V_2O_5 films, Thin Solid Films, 182 (1-2), 79-86 (1989). https://doi.org/10.1016/0040-6090(89)90245-9.
8. H. Hirashima, M. Ide, and T. Toshida, Memory switching of V_2O_5 -TeO_2 glasses, J. Non-cryst. Solids 86(3), 327-335 (1986). https://doi.org/10.1016/0022-3093(86)90021-9.
9. Tamang, R., Varghese, B., Tok, E.S., Mhaisalkar, S., Sow, C.H. (2012-07). Sub-bandgap energy photoresponse of individual V_2O_5 nanowires. Nanoscience

andNanotechnology Letters 4 (7), 716-719. https://doi.org/10.1166/nnl.2012.1381.

10. M. Abyazisani, M.M. Bagheri-Mohagheghi, M.R. Benam, Study of structural and optical properties of nanostructured V_2O_5 thin films doped with fluorine, Mater. Sci. Semicond. Process, 31 (2015) 693–699. https://doi.org/10.1016/j.mssp.2014.12.049.
11. E. Cazzanelli, G. Mariotto, S. Passerini, W. H. Smyrl, and A. Gorenstein, Raman and XPS characterization of vanadium oxide thin films deposited by reactive RF sputtering, Sol. Energy Mater. Sol. Cells 56, 249-258 (1999). https://doi.org/10.1016/S0927-0248(98)00135-4.
12. N. Ozer, Electrochemical properties of sol-gel deposited vanadium pentoxide films, Thin Solid Films 305 (1-2), 80-87 (1997). https://doi.org/10.1016/S0040-6090(97)00086-2.
13. J. Livage, vanadium pentoxide gels, Chem. Mater., 3(4) ,578-593 (1991).
14. J. Livage, Hydrothermal Synthesis of Nanostructured Vanadium Oxides Materials, 3(8), 4175-4195 (2010). https://doi.org/10.3390/ma3084175.
15. D. Barreca, L. Armelao, F. Caccavale, V. D. Noto, A. Gregori, G. A. Rizzi, and E.Tondello, Highly Oriented V_2O_5 Nanocrystalline Thin Films by Plasma-Enhanced Chemical Vapor Deposition,Chem. Mater. 2000, 12(1), 98–103. https://doi.org/10.1021/cm991095a.
16. Takeuchi, J. K.; Marschilok, A. C.; Davis, S. M.; Leising, R. A.; Takeuchi, E. S. Coord. Chem. Rev. 219-221, 283 (2001).
17. Rao M.C., Vacuum Evaporated V2O5 Thin Films for Gas Sensing Application , Int. J. Chem Tech. Res., 6(3), 1904-1906 (2014).
18. A. Bouzidi, N. Benramdane, A. Nakrela, C. Mathieu, B. Khelifa, R. Desfeux, A. Da Costa, First synthesis of vanadium oxide thin films by spray pyrolysis technique, Mater. Sci. Eng. B 95 (2), 141-147 (2002). https://doi.org/10.1016/S0921-5107(02)00224-6.
19. Alaa A. Akl, Effect of solution molarity on the characteristics of vanadium pentoxide thin film, Appl. Surf. Sci. 252 (24), 8745-8750 (2006). https://doi.org/10.1016/j.apsusc.2005.12.076
20. L. Boudaoud, N. Benramdane, R. Desfeux, B. Khelifa, C. Mathieu, Structural and optical properties of MoO3 and V2O5 thin films prepared by Spray Pyrolysis, Catal. Today 113 (3-4), 230-234 (2006). https://doi.org/10.1016/j.cattod.2005.11.072.
21. F. Abeles, Optical Properties of Solids, North Holland, Amsterdam, 303, ISBN: 044410058X (1972).
22. Yuanfang Zhang, Jialiang Huang, Pengfei Zhang, Jialin Cong, Jianjun Li and Xiaojing Hao,Formation mechanisms of voids and pin-holes in $cusbs_2$ thin film synthesized by sulfurizing a co-sputtered cu–sb precursor,J. Mater. Chem. A, 2022,10, 8015-8024. https://doi.org/10.1039/D2TA00208F.